

The glass transition and the replica symmetry breaking in vortex matter

^{1,3}Dingping Li and ^{2,3}Baruch Rosenstein

¹Department of Physics, Peking University, Beijing 100871, China, P.R.C.

²Department of Condensed Matter Physics, Weizmann Institute of Science, Rehovot 76100, Israel. and

³National Center for Theoretical Sciences and Electrophysics Department,
National Chiao Tung University, Hsinchu 30050, Taiwan, R.O.C.

(Dated: November 20, 2018)

We quantitatively describe the competition between the thermal fluctuations and the disorder using the Ginzburg – Landau approach. Flux line lattice in type II superconductors undergoes a transition into three “disordered” phases: vortex liquid (not pinned), homogeneous vortex glass (pinned) and crystalline Bragg glass (pinned) due to both thermal fluctuations and random quenched disorder. We show that disordered Ginzburg – Landau model (valid not very far from H_{c2}) in which only the coefficient of a term quadratic in order parameter ψ is random first considered by Dorsey, Fisher and Huang leads to a state with nonzero Edwards – Anderson order parameter, but this state is still replica symmetric. However when the coefficient of the quartic term $|\psi|^4$ in GL free energy also has a random component, replica symmetry breaking effects appear. The location of the glass transition line in 3D materials is determined and compared to experiments. The line is clearly different from both the melting line and the second peak line describing the translational and rotational symmetry breaking at high and low temperatures respectively. The phase diagram is therefore separated by two lines into four phases mentioned above.

PACS numbers: PACS numbers: 74.20.De, 74.60.-w, 74.25.Ha, 74.25.Dw

I. INTRODUCTION

In any superconductor there are impurities either present naturally or systematically produced using the proton or electron irradiation. The inhomogeneities both on the microscopic and the mesoscopic scale greatly affect thermodynamic and especially dynamic properties of type II superconductors in magnetic field. The magnetic field penetrates the sample in a form of Abrikosov vortices, which can be pinned by disorder. In addition thermal fluctuations also greatly influence the vortex matter in high T_c superconductors, for example in some cases thermal fluctuations will effectively reduce the effects of disorder. As a result the $H - T$ phase diagram of the high T_c superconductors is very complex due to the competition between thermal fluctuations and disorder, and it is still far from being reliably determined, even in the best studied superconductor, the optimally doped $YBCO$ superconductor.¹ Difficulties are both experimental and theoretical. Experimentally various phases with various (frequently overlapping) names like liquid² (sometimes differentiated into liquid I and liquid II³), vortex solid, Bragg glass⁴ (=pinned solid), vortex glass (=pinned liquid=entangled solid,⁵ the vortex slush⁶), were described. To differentiate various phases one should understand the nature of the phase transitions between them. Although over the years the picture has evolved with various critical and tricritical points appeared and disappeared, several facts become increasingly clear.

1. The first order^{7,8} melting line seems to merge with the “second magnetization peak” line forming the universal order - disorder phase transition line.^{9,10} At the low temperatures the location of this line strongly depends on disorder and generally exhibits a positive slope (termed also the “inverse” melting¹¹), while in the “melting” section it is dominated by thermal fluctuations and has a large negative slope. The resulting maximum at which the magnetization and the entropy jump vanish was interpreted either as a tricritical point^{3,12} or a Kauzmann point.¹³ This universal “order - disorder” transition line (ODT), which appeared first in the strongly layered superconductors ($BSCCO$ ⁹) was extended to the moderately anisotropic superconductors ($LaSCCO$ ¹⁰) and to the more isotropic ones like $YBCO$.^{13,14} The symmetry characterization of the transition is clear: spontaneous breaking of the translation and rotation symmetry.

2. The universal “order - disorder” line is different from the “irreversibility line” or the “glass” transition (GT) line, which is a continuous transition.^{15,16} The almost vertical glass line clearly represents effects of disorder although the thermal fluctuations affect the location of the transition. Experiments in $BSCCO$ ¹⁷ indicate that the line crosses the ODT line right at its maximum, continues deep into the ordered (Bragg) phase. This proximity of the glass line to the Kauzmann point is reasonable since both signal the region of close competition of the disorder and the thermal fluctuations effects. In more isotropic materials the data are more confusing. In $LaSCCO$ ¹⁸ the GT line is closer to the “melting” section of the ODT line still crossing it. In $YBCO$ we are not aware of a claim that the GT line continuous into the ordered phase. Most of experiments¹² indicate that the GT line terminates at the “tricritical point” in the vicinity of the maximum of the ODT line. It is more difficult to characterize the nature of the GT transition as a “symmetry breaking”. The common wisdom is that “replica” symmetry is broken in the glass (either

via "steps" or via "hierarchical" continuous process) as in the most of the spin glasses theories.¹⁹

Theoretically the problem of the vortex matter subject to thermal fluctuations or disorder has a long history. An obvious candidate to model the disorder is the Ginzburg - Landau model in which coefficients have random components. However this model is too complicated and simplifications are required. The original idea of the vortex glass and the continuous glass transition exhibiting the glass scaling of conductivity diverging in the glass phase appeared early in the framework of the frustrated XY model (the gauge glass).^{20,21} In this approach one fixes the amplitude of the order parameter retaining the magnetic field with random component added to the vector potential. It was studied by the RG and the variational methods and has been extensively simulated numerically.^{6,22} In analogy to the theory of spin glass the replica symmetry is broken when crossing the GT line. The model ran into several problems (see Giamarchi and Bhattacharya in Ref. 23 for a review): for finite penetration depth λ it has no transition²⁴ and there was a difficulty to explain sharp Bragg peaks observed in the experiments at low magnetic fields. To address the last problem another simplified model had been proven to be more convenient: the elastic medium approach to a collection of interacting line-like objects subject to both the pinning potential and the thermal bath Langevin force.^{25,26} The resulting theory was treated again using the gaussian approximation^{4,27} and RG.²¹ The result was that in $2 < D < 4$ there is a transition to a glassy phase in which the replica symmetry is broken following the "hierarchical pattern" (in $D = 2$ the breaking is "one step"). The problem of the very fast destruction of the vortex lattice by disorder was solved with the vortex matter being in the replica symmetry broken (RSB) phase and it was termed "Bragg glass".⁴ It is possible to address the problem of mesoscopic fluctuation using an approach in which one directly simulates the interacting line-like objects subject to both the pinning potential and the thermal bath Langevin force.^{25,26} In this context the generalized replicated density functional theory²⁸ was also applied resulting in one step RSB solution. Although the above approximations to the disordered GL theory are very useful in more "fluctuating" superconductors like $BSCCO$, a problem arises with their application to $YBCO$ at temperature close T_c (where most of the experiments mentioned above are done): vortices are far from being line-like and even their cores significantly overlap. As a consequence the behavior of the dense vortex matter is expected to be different from that of a system of pointlike vortices and of the XY model although the elastic medium approximation might still be meaningful.²⁹

To describe the non-pointlike vortices, one has to return to the GL model and make a different simplification. One of the most developed schemes is the lowest Landau level (LLL) approximation valid close to the $H_{c2}(T)$ line.³⁰ Such an attempt was made by Dorsey, Fisher and Huang³¹ in the liquid phase using the dynamic approach³² and by Tesanovic and Herbut for columnar defects in layered materials using supersymmetry.³³ It is the purpose of this paper to study the glass transition using the replica formalism. We quantitatively study the glass transition in the same model, with the disorder represented by the random component of the coefficients of the GL free energy. The most general hierarchical homogeneous (liquid) Ansatz³⁴ and its stability are considered to obtain the glass transition line and to determine the nature of the transition for various values of the disorder strength of the GL coefficients. Then we place the glass line on the phase diagram of $YBCO$ and compare with experiments and other theories.

The paper is organized as follows. The general disordered GL model is introduced in section II and the gaussian variational replica method is presented in section III. Next we study in some detail the model either with $|\psi|^2$ disorder in Section IV, with less details the $|\psi|^4$ disorder in Section V and obtain the phase transition lines in those two cases. In Section VI, the general model containing both the $|\psi|^2$ disorder and the $|\psi|^4$ disorder is treated briefly. In Section VII, we compare our results with the experimental data and conclude in section VIII by summarizing our results.

II. DISORDER EFFECTS IN THE GINZBURG - LANDAU DESCRIPTION OF THE TYPE II SUPERCONDUCTOR

A. Ginzburg - Landau free energy

We start from the Gibbs energy of the ideal homogeneous sample (no disorder):

$$G = \int dx^3 \frac{\hbar^2}{2m_{||}^*} |\partial_z \psi|^2 + \frac{\hbar^2}{2m_{\perp}^*} |\vec{D}\psi|^2 + a' \psi^* \psi + \frac{b'}{2} (\psi^* \psi)^2 + \frac{(H - B)^2}{8\pi}. \quad (1)$$

Here $a' = \alpha(T - T_c)$ and b' are constant parameters, $\vec{D} \equiv (-i\hbar \nabla + \frac{e^*}{c} \vec{A})$ is the covariant derivative, \vec{A} is the vector potential, the magnetic field $\vec{B} = \nabla \times \vec{A}$, H is the external magnetic field, m_{\perp}^* and $m_{||}^*$ are the effective masses in directions perpendicular and parallel to the field respectively. Mesoscopic thermal fluctuations are accounted for via

Boltzmann weights

$$Z = \int_{\psi^*, \psi} \exp \left\{ -\frac{G[\psi^*, \psi]}{T} \right\} \quad (2)$$

The model provides a good description of thermal fluctuations as long as $1 - t - b \ll 1$, where $t = \frac{T}{T_c}$, $b = B/H_{c2}$ ($h = H/H_{c2}$), $H_{c2} = \Phi_0/(2\pi\xi^2)$ and ξ is the coherence length. In this case the higher order terms like $|\psi|^6$ can be omitted (detail notation can be found in Ref. 35). The 3D GL model describes materials with not too high anisotropy (for a recent evidence of validity of this assumption in $YBCO$ see Ref. 36). In strongly anisotropic materials, a model of the Lawrence – Doniach type is more appropriate.³⁷

Within the GL approach the pointlike quenched disorder on the mesoscopic scale is described by making **each** of the coefficients of the mesoscopic GL energy a random value centered around a certain constant value given in eq. (2). For example effective masses can be disordered

$$\frac{m_{\perp}^{*-1}}{U(x)U(y)} \rightarrow \frac{m_{\perp}^{*-1}(1 + U(x))}{U(x)U(y)} = P\delta(x - y). \quad (3)$$

The parallel effective mass m_{\parallel}^* might also have the random component which we neglect (it is relatively small since m_{\parallel}^* is typically very large), though it can be incorporated with no additional difficulties. This type of disorder is sometimes called the δl disorder since it originates in part from the inhomogeneity of the electron mean free path l in Gor'kov's derivation. From the BCS theory, effective mass is $m^* = 2m_e \left(1 + \frac{\pi^3 \hbar v_F}{168\zeta(3)T_c l}\right)$ in the clean limit and $m^* = 2m_e \frac{7\zeta(3)\hbar v_F}{2\pi^3 T_c l}$ in the dirty limit. Relation to the notations of Ref. 37 (chapter II in this reference) is the following: U is $-\delta m_{ab}/m_{ab}$ and $P = \gamma_m/m_{ab}^2$. Note however that, in addition to the random distribution of l , disorder in v_F and T_c (the density of states and interaction strength) can also affect m^* .

The other two parameters in the GL equations are $\alpha = \frac{12\pi^2 T_c}{7\zeta(3)\epsilon_F}$ and $b' = \frac{18\pi^2}{7\zeta(3)N\epsilon_F} \left(\frac{T_c}{\epsilon_F}\right)^2$. The coefficient of the quadratic term is called δT disorder since it describes a local deviation of the critical temperature. Introducing a random component in $|\psi|^2$ term:

$$a' \rightarrow a'(1 + W(x)); \quad \overline{W(x)W(y)} = R\delta(x - y). \quad (4)$$

In notations of Ref. 37 the random field $W(x) = -\delta_a/a$, $R = \gamma_a/a^2$. When thermal fluctuations of the vortex degrees of freedom can be neglected, these two random fields would be sufficient (they control the two relevant scales ξ and λ). The reason is that one can set the coefficient of the third term $|\psi|^4$ to a constant by rescaling. However in the presence of thermal fluctuations the coefficient of $|\psi|^4$ also should be considered as having a random component. It cannot be “rescaled out” since it affects the Boltzmann weights. We will see later that at least within the lowest Landau level approximation this term is crucial in inducing certain glassy properties of the vortex matter state. We therefore introduce its disorder via

$$b' \rightarrow b'(1 + V(x)); \quad \overline{V(x)V(y)} = Q\delta(x - y). \quad (5)$$

In unconventional superconductors, even without disorder, the phenomenological GL model has not been reliably derived microscopically. The coefficients and their inhomogeneities therefore should be considered as phenomenological parameters to be fitted to experiments. We assume that U , R and Q have weak dependencies on field and temperature. The assumption of the weak temperature and field dependence of the disorder strengths U , R and Q , as that of any parameter in the GL approach, should be derived in principal from a microscopic theory assuming random chemical potential or should be justified by fitting to experiments. For simplicity the white noise distribution is considered

$$p[U, W, V] = \exp \left[- \int_x \frac{U(x)^2}{2P} + \frac{W(x)^2}{2R} + \frac{V(x)^2}{2Q} \right]$$

for random components. The free energy of superconductor after averaging over the disorder is

$$\overline{F} = -\frac{T}{norm} \int_{U, W, V} p[U, W, V] \log \left[\int_{\psi} \exp[-g[\psi] - f_{dis}[U, W, V, \psi]] \right]; \quad (6)$$

$$g = G/T; \quad f_{dis}[U, W, V, \psi] = \frac{1}{T} \int_x \frac{\hbar^2}{2m_{\perp}^*} U(x) \left| \vec{D}\psi \right|^2 + a' W(x) |\psi|^2 + \frac{1}{2} V(x) |\psi|^4, \quad (7)$$

where $norm \equiv \int_{U,W,V} p[U, W, V]$ is a normalization factor.

To make the physical picture clear, we rescale the coordinates as $x \rightarrow \xi x$, $y \rightarrow \xi y$, $z \rightarrow \frac{\xi z}{\gamma}$ with anisotropy parameter defined by $\gamma = (m_{||}^*/m_{\perp}^*)^{1/2}$. The order parameter is scaled as $\psi^2 \rightarrow \frac{2\alpha T_c}{b'} \psi^2$. The dimensionless free energy becomes simpler looking:

$$g[\psi] = G/T = \frac{1}{\omega} \int_x \frac{1}{2} |\partial_z \psi|^2 + \frac{1}{2} |\vec{D}\psi|^2 + \frac{t-1}{2} |\psi|^2 + \frac{1}{2} |\psi|^4 + \frac{\kappa^2 (b-h)^2}{4}, \quad (8)$$

where $\omega = \sqrt{2Gi\pi^2 t}$. The Ginzburg number is $Gi \equiv 32 [\pi\lambda^2 T_c \gamma / (\Phi_0^2 \xi)]^2$, where λ is the magnetic penetration depth. The last term can be ignored in calculating \overline{F} as the κ is very big in high T_c superconductors and the last term is order of $\frac{1}{\kappa^2}$. Similarly the random component and the distribution become:

$$f_{dis}[U, W, V, \psi] = \frac{1}{\omega} \int_x \left\{ -\frac{1}{2} U(x) \psi^* D^2 \psi + \frac{t-1}{2} W(x) |\psi|^2 + \frac{1}{2} V(x) |\psi|^4 \right\} \quad (9)$$

$$p[U, W, V] = \exp \left[-\frac{\xi^3}{\gamma} \int_x \left(\frac{U(x)^2}{2P} + \frac{W(x)^2}{2R} + \frac{V(x)^2}{2Q} \right) \right]. \quad (10)$$

The model however is highly nontrivial even without disorder, and to make progress, further approximation is needed.

B. Lowest Landau level approximation

The lowest Landau level (LLL) approximation³⁰ is based on constraint $-D^2\psi = b\psi$. Over the years this model has been studied by various methods, analytic and numerical.^{35,38,39} The (effective) LLL model is applicable in a surprisingly wide range of fields and temperatures determined by the condition that the relevant excitation energy ε is much smaller than the gap between Landau levels $2\hbar eB/(cm_{\perp})$.¹³

The free energy after further rescaling $x \rightarrow x/\sqrt{b}$, $y \rightarrow y/\sqrt{b}$, $z \rightarrow z \left(\frac{2^{5/2}\pi}{b\omega} \right)^{1/3}$, $\psi^2 \rightarrow \left(\frac{2^{5/2}\pi}{b\omega} \right)^{2/3} \psi^2$, simplifies within the LLL approximation to:

$$f_{LLL} = \frac{1}{2^{5/2}\pi} \int d^3x \left[\frac{1}{2} |\partial_z \psi|^2 + a_T |\psi|^2 + \frac{1}{2} |\psi|^4 \right]. \quad (11)$$

Not surprisingly the number of independent constants in LLL is one less than in the general model. This fact leads to the “LLL scaling” relations (of course the disorder terms will break LLL scaling). As a result the simplified model without disorder has just one parameter – the (dimensionless) scaled temperature:

$$a_T = - \left(\frac{2\pi}{b\omega} \right)^{2/3} (1 - t - b). \quad (12a)$$

The disorder term becomes:

$$f_{LLL}^{dis} = \frac{1}{2^{5/2}\pi} \int d^3x \left\{ \Omega(x) |\psi|^2 + \frac{1}{2} V(x) |\psi|^4 \right\}, \quad (13)$$

in which only combination of W and U enters $\Omega(x) = \frac{1}{2} \left[2(t-1) \left(\frac{2\pi}{b\omega} \right)^{2/3} W(x) - bU(x) \right]$. Its distribution is still gaussian

$$\overline{p}(\Omega, V) = \exp \left[- \int_x \frac{\Omega(x)^2}{2r'} + \frac{V(x)^2}{2q} \right] \quad (14)$$

with two variances

$$r' = \frac{\gamma}{4\sqrt{2}\xi^3} \left\{ \frac{8\pi}{\omega} (1-t)^2 R + \left(\frac{b^2\omega}{2\pi} \right)^{1/3} b^2 P \right\} \quad (15)$$

$$q' = \frac{\gamma}{\sqrt{2}\xi^3} \left(\frac{b^2\omega}{2\pi} \right)^{1/3} Q.$$

To treat both the thermal fluctuations and disorder we will use the replica method to integrate over impurity distribution followed by gaussian approximation.

III. REPLICA TRICK AND GAUSSIAN APPROXIMATION

A. Replica trick

We will use the replica trick to evaluate the disorder averages. The replica method is widely used to study disordered electrons in the theory of spin glasses,¹⁹ disordered metals and was applied to vortex matter in the London limit.^{27,40} Applying a simple mathematical identity to the disorder average of the free energy one obtains:

$$\overline{F} = \overline{-T \lim_{n \rightarrow 0} \frac{1}{n} (Z^n - 1)}. \quad (16)$$

The averages of Z^n is the statistical sum over n identical "replica" fields ψ_a , $a = 1, \dots, n$:

$$\overline{Z^n} = \frac{1}{norm} \int_{\Omega, V} p[\Omega, V] \prod_a \int_{\psi_a} \exp \{-f[\psi_a] - f_{dis}[\Omega, V, \psi_a]\}. \quad (17)$$

The integral over the disorder potential is gaussian and results in:

$$\begin{aligned} \overline{Z^n} &= \int_{\psi_a} \exp \left[- \sum_a f(\psi_a) + \frac{1}{2(2^{5/2}\pi)^2} \sum_{a,b} f_{ab} \right] \\ f_{ab} &= r' |\psi_a|^2 |\psi_b|^2 + \frac{q'}{4} (\psi_a^* \psi_a)^2 (\psi_b^* \psi_b)^2. \end{aligned} \quad (18)$$

This model is a type of scalar field theory and the simplest nonperturbative scheme commonly used to treat such a model is gaussian approximation. Its validity and precision can be checked only by calculating corrections.

B. Gaussian approximation

We have assumed that the order parameter is constrained to the LLL and therefore can be expanded in a basis of the standard LLL eigenfunctions in Landau gauge:

$$\psi_a(x) = norm \int_{k_z, k} e^{i(zk_z + xk)} \exp \left\{ -\frac{1}{2}(y + k)^2 \right\} \tilde{\psi}_a(k). \quad (19)$$

We now apply the gaussian approximation which has been used in disorder in the elastic medium approach,^{27,40} following its use in polymer physics.⁴¹ The gaussian approximation was applied to the vortex liquid within the GL approach in 30,39. The gaussian effective free energy is expressed via variational parameter^{35,41} μ_{ab} which in the present case is a matrix in the replica space. The correlator is parametrized as

$$\langle \psi_a^*(k, k_z) \psi_b(-k, -k_z) \rangle = G_{ab}(k_z) = \frac{2^{5/2}\pi}{\frac{k_z^2}{2} \delta_{ab} + \mu_{ab}^2} \quad (20)$$

The bubble integral appearing in the free energy is very simple:

$$\langle \psi_a^*(x, y, z) \psi_b(x, y, z) \rangle = \frac{\sqrt{2}}{\pi} \int_{k_z} \frac{1}{\frac{k_z^2}{2} \delta_{ab} + \mu_{ab}^2} = 2\mu_{ab}^{-1} \equiv 2m_{ab}.$$

As a result the gaussian effective free energy can be written in a form:

$$\begin{aligned}
n f_{eff} &= \sum_a \left\{ \frac{2^{5/2}\pi}{(2\pi)^3} \int_{k_z} \left[\text{Log}G^{-1}(k_z) + \left(\frac{k_z^2}{2} + a_T \right) G(k_z) - I \right]_{aa} + 4(m_{aa})^2 \right\} \\
&\quad - \sum_{a,b} \left\{ \frac{1}{2^{3/2}\pi} r' |m_{ab}|^2 + \frac{\sqrt{2}}{\pi} q' \left(|m_{ab}|^4 + 4m_{aa}m_{bb} |m_{ab}|^2 \right) \right\} \\
&= 2 \sum_a \left\{ \mu_{aa} + a_T m_{aa} + 2(m_{aa})^2 \right\} \\
&\quad - 2 \sum_{a,b} \left\{ r |m_{ab}|^2 + q \left(\frac{1}{4} |m_{ab}|^4 + m_{aa}m_{bb} |m_{ab}|^2 \right) \right\},
\end{aligned} \tag{21}$$

where we discarded an (ultraviolet divergent) constant and renormalization of a_T and rescaled the disorder strength: $r = \frac{1}{2^{5/2}\pi} r'$, $q = \frac{2^{5/2}}{\pi} q'$.

We start with a simple case in which only the $|\psi|^2$ type of disorder is present. More precisely we take $q = 0$ and return to the general case in section IV. This model has been already discussed using different method (the Sompolinsky dynamic approach) in the unpinned phase in Ref. 31.

IV. NONZERO EDWARDS - ANDERSON ORDER PARAMETER AND ABSENCE OF THE REPLICA SYMMETRY BREAKING WHEN ONLY THE $|\psi|^2$ DISORDER IS PRESENT

A. Hierarchical matrices and impossibility of the continuous replica symmetry breaking

In this section we neglect the $|\psi|^4$ disorder term. It is convenient to introduce real (not necessarily symmetric) matrix Q_{ab} , which is in one to one linear correspondence with Hermitian (generally complex) matrix m_{ab} via

$$Q_{ab} = \text{re}[m_{ab}] + \text{im}[m_{ab}]. \tag{22}$$

Unlike m_{ab} , all the matrix elements of Q_{ab} are independent. In terms of this matrix the free energy can be written as

$$\frac{n}{2} f_{eff} = \sum_a \left\{ (m^{-1})_{aa} + a_T Q_{aa} + 2(Q_{aa})^2 \right\} - r \sum_{a,b} Q_{ab}^2. \tag{23}$$

Taking derivative with respect to Q_{ab} gives the saddle point equation for this matrix element:

$$\frac{n}{2} \frac{\delta f}{\delta Q_{ab}} = -\frac{1}{2} \left[(1-i)(m^{-2})_{ab} + c.c. \right] + a_T \delta_{ab} + 4Q_{aa} \delta_{ab} - 2rQ_{ab} = 0. \tag{24}$$

Since the electric charge (or the superconducting phase) $U(1)$ symmetry is assumed, we consider only solutions with real m_{ab} . In this case $m_{ab} = Q_{ab}$ is a symmetric real matrix. General hierarchical matrices m are parametrized using the diagonal elements \tilde{m} and the Parisi's (monotonically increasing) function m_x specifying the off diagonal elements with $0 < x < 1$.⁴¹ Physically different x represent time scales in the glass phase. In particular the Edwards - Anderson (EA) order parameter is $m_{x=1} = M > 0$.

A nonzero value for this order parameter signals that the annealed and the quenched averages are different. The dynamic properties of such phase are generally quite different from those of the nonglassy $M = 0$ phase. In particular it is expected to exhibit infinite conductivity.^{20,31} We will refer to this phase as the "ergodic pinned liquid" (EPL) distinguished from the "nonergodic pinned liquid" (NPL) in which, in addition, the ergodicity is broken.

However in the present model RSB does not occur. In terms of Parisi parameter \tilde{m} and m_x the matrix equation eq.(24) takes a form:

$$-\widetilde{m^{-2}} + a_T + (4 - 2r) \tilde{m} = 0 \tag{25}$$

$$(m^{-2})_x + 2rm_x = 0.$$

Dynamically if m_x is a constant, pinning does not result in the multitude of time scales. Certain time scale sensitive phenomena like various memory effects⁴² and the responses to “shaking”¹¹ are expected to be different from the case when m_x takes multiple values. If m_x takes a finite different number of n values, we call $n - 1$ step RSB. On the other hand, if m_x is continuous, the continuous replica symmetry breaking (RSB) occurs.

In order to show that m_x is a constant, it is convenient to rewrite the second equation via the matrix μ , the matrix inverse to m :

$$(\mu^2)_x + 2r(\mu^{-1})_x = 0. \quad (26)$$

Differentiating this equation with respect to x one obtains;

$$2 \left[\{\mu\}_x - r (\{\mu\}_x)^{-2} \right] x \frac{d\mu_x}{dx} = 0, \quad (27)$$

where we used a set of standard notations in the spin glass theory:⁴¹

$$\{\mu\}_x \equiv \tilde{\mu} - \langle \mu_x \rangle - [\mu]_x; \quad \langle \mu_x \rangle \equiv \int_0^1 dx \mu_x; \quad [\mu]_x = \int_0^x dy (\mu_x - \mu_y). \quad (28)$$

If one is interested in a continuous monotonic part $\frac{d\mu_x}{dx} \neq 0$, the only solution of eq.(27) is

$$\{\mu\}_x = r^{1/3} \quad (29)$$

Differentiating this again and dropping the nonzero derivative $\frac{d\mu_x}{dx}$ again, one further gets a contradiction: $\frac{d\mu_x}{dx} = 0$. This proves that there are no such monotonically increasing continuous segments. One can therefore generally have either the replica symmetric solutions, namely $m_x = M$ or look for a several steplike RSB solutions.¹⁹ We can show that the constant m_x solution is stable. Therefore, if a steplike RSB solution exists, it might be only an additional local minimum. We explicitly looked for a one step solution and found that there is none.

B. Two replica symmetric solutions and the third order transition between them

1. The unpinned liquid and the “ergodic glass” replica symmetric solutions

Restricting to RS solutions, $m_x = M$, the saddle point equations eq.(25) simplify:

$$\begin{aligned} -\varepsilon^{-2} + (a_T + 4\tilde{m}) - 2r\varepsilon &= 0; \\ M(\varepsilon^{-3} - r) &= 0, \end{aligned} \quad (30)$$

where $\varepsilon \equiv \tilde{m} - M$. Energy of such a solution is given by

$$\frac{f_{eff}}{2} = 2\varepsilon^{-1} - 2 - \varepsilon^{-2}M + 2a_T\tilde{m} + 4\tilde{m}^2 - 2r(\varepsilon^2 + 2\varepsilon M). \quad (31)$$

The second equation eq.(30) has a replica index independent (diagonal) solution $M = 0$. In addition there is a non diagonal one. It turns out that there is a third order transition between them.

For the diagonal solution $\varepsilon = \tilde{m}$ and the first equation is just a cubic equation:

$$-\tilde{m}^{-2} + (a_T + 4\tilde{m}) - 2r\tilde{m} = 0. \quad (32)$$

For the non diagonal solution the second equation gives $\varepsilon = r^{1/3}$, which, when plugged into the first equation, gives:

$$\tilde{m} = \frac{1}{4} (3r^{2/3} - a_T); \quad M = \frac{1}{4} (3r^{2/3} - a_T) - r^{-1/3}. \quad (33)$$

The matrix m therefore is

$$m_{ab} = r^{-1/3} \delta_{ab} + M, \quad (34)$$

which results in the following value of the free energy: $f = 6r^{1/3} - \frac{1}{4}(3r^{2/3} - a_T)^2$.

The two solutions coincide for

$$a_T = r^{-1/3}(3r - 4). \quad (35)$$

Since in addition to the energy, the first and second derivatives of the energy, $\frac{df}{da_T} = 2r^{-1/3}$ and $\frac{d^2f}{da_T^2} = -\frac{1}{2}$ respectively, coincide (the fourth derivatives are different though), the transition is a third order one.

2. Stability domains of the two solutions

In order to prove that a solution is stable beyond the set of replica symmetric matrices m one has to calculate the second derivative of free energy (called Hessian in Refs. 19,43) with respect to arbitrary real matrix Q_{ab} defined in eq.(22):

$$\begin{aligned} H_{(ab)(cd)} &= \frac{n}{2} \frac{\delta^2 f_{eff}}{\delta Q_{ab} \delta Q_{cd}} \\ &= \frac{1}{2} [(m^{-2})_{ac} (m^{-1})_{db} - i (m^{-2})_{ad} (m^{-1})_{cb}] + \\ &\quad \frac{1}{2} [(m^{-1})_{ac} (m^{-2})_{db} - i (m^{-1})_{ad} (m^{-2})_{cb}] + cc \\ &\quad + 4\delta_{ac}\delta_{bd}\delta_{ab} - 2r\delta_{ac}\delta_{bd}. \end{aligned} \quad (36)$$

We will use a simplified notation for the product of the Kronecker delta functions with more than two indices: $\delta_{ac}\delta_{bd}\delta_{ab} \equiv \delta_{abcd}$. For the diagonal solution the Hessian is a very simple operator on the space of real symmetric matrices:

$$H_{(ab)(cd)} = c_I I_{abcd} + c_J J_{abcd}, \quad (37)$$

where the operators I (the identity in this space) and J are defined as

$$I \equiv \delta_{ac}\delta_{bd}; \quad J = \delta_{abcd} \quad (38)$$

and their coefficients in the diagonal phase are:

$$c_I = 2(\tilde{m}^{-3} - r), \quad c_J = 4 \quad (39)$$

with \tilde{m} being a solution of eq.(32). The corresponding eigenvectors in the space of symmetric matrices are $v_{(cd)} \equiv A\delta_{cd} + B$. To find eigenvalues λ of H we apply the Hessian on V . The result is (dropping terms vanishing in the limit $n \rightarrow 0$):

$$H_{(ab)(cd)} v_{cd} = A(c_I + c_J)\delta_{ab} + B(c_I + c_J\delta_{ab}) = \lambda(A\delta_{ab} + B) \quad (40)$$

There two eigenvalues: $\lambda^{(1)} = c_I$ and $\lambda^{(2)} = c_I + c_J$. Since $c_J = 4 > 0$, the sufficient condition for stability is:

$$c_I = 2(\tilde{m}^{-3} - r) > 0. \quad (41)$$

It is satisfied everywhere below the transition line of eq.(35), see Fig 1. (a_T, r phase diagram). The analysis of stability of the non diagonal solution is slightly more complicated. The Hessian for the non diagonal solution is:

$$H_{(ab)(cd)} = c_V V + c_U U + c_J J, \quad (42)$$

where new operators are

$$V_{(ab)(cd)} = \delta_{ac} + \delta_{bd}; U_{(ab)(cd)} = 1 \quad (43)$$

and coefficients are

$$c_V = -3Mr^{2/3}; \quad c_U = 4M^2r^{1/3}; \quad c_J = 4 \quad (44)$$

In the present case, one obtains three different eigenvalues,^{19,43} $\lambda^{(1,2)} = 2 \left(1 \pm \sqrt{1 - 4Mr^{2/3}} \right)$ and $\lambda^{(3)} = 0$. Note that the eigenvalue of Hessian on the antisymmetric matrices are degenerate with eigenvalue $\lambda^{(1)}$ in this case (we will come back later on this eigenvalue). For $M < 0$ the solution is unstable due to negative $\lambda^{(2)}$. For $M > 0$, both eigenvalues are positive and the solution is stable. The line $M = 0$ coincides with the third order transition line, hence the non diagonal solution is stable when the diagonal is unstable and *vise versa*. We conclude that there is no glass state in the vortex liquid without the $|\psi|^4$ disorder term. The transition does not correspond to RSB. Despite this in the phase with nonzero EA (NEA) M order parameter there are Goldstone bosons corresponding to $\lambda^{(3)}$ in the replica limit of $n \rightarrow 0$. The criticality and the zero modes due to disorder (pinning) in this phase might lead to great variety of interesting phenomena in statics and dynamics. These have not been explored yet. However, as we show in the next section, the random component of the quartic term changes the character of the transition line: the replica symmetry is broken on the one side of the line. For simplicity in the next section, we consider first a case with a random component of $|\psi|^4$ and no random component of $|\psi|^2$, and return to the general case in section V.

V. THE GLASS TRANSITION FOR THE $|\psi|^4$ DISORDER

A. Continuous replica symmetry breaking solutions

In this section we neglect the $r|\psi|^2$ term disorder. Although it is always present, as we have seen in the previous section, at least within the gaussian approximation, it does not cause replica symmetry breaking. Therefore one expects that although it certainly influences properties of the vortex matter, for example, the melting transition line to lower fields and temperatures,¹³ its role in qualitative understanding of RSB effects is minor. The only other disordered term within the LLL approximation considered in this paper is the $|\psi|^4$ disorder term. As was discussed in section II, at least within the BCS theory, it is expected to be smaller than the $|\psi|^2$ disorder, $q \ll r$. Even it could be very small, however, as we show here, it leads to qualitatively new phenomena in vortex matter. The $r = 0$ free energy after integration over k_z becomes:

$$\frac{n}{2} f_{eff} = \sum_a \left\{ (m^{-1})_{aa} + a_T m_{aa} + 2(m_{aa})^2 \right\} - q \sum_{a,b} \left(\frac{1}{4} |m_{ab}|^4 + m_{aa} m_{bb} |m_{ab}|^2 \right) \quad (45)$$

In terms of the real matrix Q_{ab} defined in eq.(22) the free energy can be written as

$$\frac{n}{2} f_{eff} = \sum_a \left\{ (m^{-1})_{aa} + a_T Q_{aa} + 2(Q_{aa})^2 \right\} \quad (46)$$

$$-q \sum_{a,b} \left(\frac{1}{8} Q_{ab}^4 + \frac{1}{8} Q_{ab}^2 Q_{ba}^2 + Q_{aa} Q_{bb} Q_{ab}^2 \right) \quad (47)$$

Taking a derivative with respect to Q_{ab} gives the saddle point equation for this matrix:

$$\frac{n}{2} \frac{\delta f}{\delta Q_{ab}} = \left[\begin{array}{c} -\frac{1}{2} [(1-i)(m^{-2})_{ab} + cc] + a_T \delta_{ab} + 4Q_{aa} \delta_{ab} \\ -q \left(\frac{1}{2} Q_{ab}^3 + \frac{1}{2} Q_{ab} Q_{ba}^2 + 2Q_{ab} Q_{aa} Q_{bb} + \delta_{ab} \sum_e Q_{ee} (Q_{ae}^2 + Q_{ea}^2) \right) \end{array} \right] = 0 \quad (48)$$

Using the hierarchical symmetric matrix parametrization of its symmetric part (the antisymmetric will not be important for most of our purposes), it takes a form

$$-\widetilde{m}^{-2} + a_T + 4\widetilde{m} - q \left(3\widetilde{m}^3 + 2\widetilde{m}^2 \widetilde{m} \right) = 0 \quad (49)$$

$$(m^{-2})_x + q(m_x^3 + 2\tilde{m}^2 m_x) = 0. \quad (50)$$

As in the previous section, it is convenient to rewrite the second equation in terms of μ , the inverse matrix of m :

$$(\mu^2)_x + q \left[((\mu^{-1})_x)^3 + 2\tilde{m}^2 (\mu^{-1})_x \right] = 0. \quad (51)$$

Differentiation of this equation with respect to x leads to:

$$\left\{ 2\{\mu\}_x - q \left[3((\mu^{-1})_x)^2 + 2\tilde{m}^2 \right] (\{\mu\}_x)^{-2} \right\} x \frac{d\mu_x}{dx} = 0. \quad (52)$$

For a continuous segment $\frac{d\mu_x}{dx} \neq 0$ one solves eq.(52) for $(\mu^{-1})_x$ in terms of $\{\mu\}_x$ getting now a more complicated result:

$$(\mu^{-1})_x = \sqrt{\frac{2}{3} \left[q^{-1} (\{\mu\}_x)^3 - \tilde{m}^2 \right]} \quad (53)$$

Differentiating this equation with respect to x again one obtains:

$$\frac{1}{(\{\mu\}_x)^2} = \sqrt{\frac{2}{3q \left[(\{\mu\}_x)^3 - q\tilde{m}^2 \right]} (\{\mu\}_x)^2 x}. \quad (54)$$

Instead of solving this for $\{\mu\}_x$ we present x as function of $\{\mu\}_x$:

$$x = \sqrt{\frac{3q \left[(\{\mu\}_x)^3 - q\tilde{m}^2 \right]}{2 (\{\mu\}_x)^8}}. \quad (55)$$

Thus the solution will be given by eq.(55) in the segment if $\frac{d\mu_x}{dx} \neq 0$ and constant μ_x in the other segments. In principle this would allow for a numerical solution. One could actually solve the equation near the transition line using the method in Ref. 34. The situation is completely different compared to that of the $|\psi|^2$ disorder. In the present case a stable RSB solution exists. We will turn first however to the replica symmetric solutions and determine their region of stability. In the unstable region of the replica symmetric solutions, the RSB solution of eq.(55) will be the relevant one.

B. Two replica symmetric solutions

1. Solutions

Here we briefly repeat the steps leading to the RS solutions for the $|\psi|^2$ disorder omitting details. The saddle point equations eq.(25) for the RS matrices $m_x = M$ are:

$$-\varepsilon^{-2} + (a_T + 4\tilde{m}) - q [5\tilde{m}^3 - M^3 - 2M^2\tilde{m} - 2\tilde{m}^2M] = 0 \quad (56)$$

$$M [2\varepsilon^{-3} - q (M^2 + 2\tilde{m}^2)] = 0 \quad (57)$$

where $\varepsilon \equiv \tilde{m} - M$. Energy of such a solution is given by

$$\frac{f}{2} = \varepsilon^{-1} - \varepsilon^{-2}M + a_T\tilde{m} + 2\tilde{m}^2 - \frac{q}{4} (5\tilde{m}^2 - M^2) (\tilde{m}^2 + M^2). \quad (58)$$

For the diagonal solution $M = 0$, $\varepsilon = \tilde{m}$ and the first equation takes a form:

$$-\tilde{m}^{-2} + a_T + 4\tilde{m} - 5q\tilde{m}^3 = 0. \quad (59)$$

The non diagonal solution in the present case is more complicated, but the condition determining the transition line between the two (equivalently the appearance of the nonvanishing EA order parameter) is still very simple: $\varepsilon = q^{-1/5}$ as $M = 0$ on the line. Along the line the scaled temperature is:

$$a_T^d = 2(3q^{2/5} - 2q^{-1/5}). \quad (60)$$

It is still the third order transition line similar to the $|\psi|^2$ disorder case and one has zero modes in NEA sector, while no such modes exist in the $M = 0$ phase. The stability analysis with respect to configurations which are replica symmetric however gives completely different results compared to that of the $|\psi|^2$ disorder.

2. Stability region of the RS solutions.

The Hessian now has several additional terms

$$H_{(ab)(cd)} \equiv \frac{n}{2} \frac{\delta^2 f}{\delta m_{ab} \delta m_{cd}} = (m^{-2})_{ac} (m^{-1})_{db} + (m^{-1})_{ac} (m^{-2})_{db} + 4\delta_{abcd} \quad (61)$$

$$-q \left(\begin{array}{l} \frac{3}{2}\delta_{ac}\delta_{bd}Q_{ab}^2 + \frac{1}{2}(\delta_{ac}\delta_{bd}Q_{ba}^2 + 2\delta_{ad}\delta_{bc}Q_{ab}Q_{ba}) \\ 2(\delta_{ac}\delta_{bd}Q_{aa}Q_{bb} + \delta_{bcd}Q_{ab}Q_{aa} + \delta_{acd}Q_{ab}Q_{bb}) \\ + \delta_{ab}[\delta_{cd}(Q_{ac}^2 + Q_{ca}^2) + 2(\delta_{ac}Q_{ad}Q_{dd} + \delta_{ad}Q_{ca}Q_{cc})] \end{array} \right)$$

For replica symmetric solutions $Q_{ab} = m_{ab} = \varepsilon\delta_{ab} + M$ the Hessian can be represented as

$$H = c_+I_+ + c_-I_- + c_UU + c_VV + c_JJ + c_KK + c_NN, \quad (62)$$

where new operators I_{\pm} , K, N are defined as

$$I_{\pm} \equiv \frac{1}{2}(\delta_{ac}\delta_{bd} \pm \delta_{ad}\delta_{bc}); \quad K \equiv \delta_{ab}\delta_{cd}; \quad N = \delta_{abc} + \delta_{abd} + \delta_{acd} + \delta_{bcd}. \quad (63)$$

The coefficients are

$$\begin{aligned} c_+ &= 2\varepsilon^{-3} - q(3M^2 + 2\tilde{m}^2); \\ c_- &= 2\varepsilon^{-3} - q(M^2 + 2\tilde{m}^2); \\ c_U &= 4M^2\varepsilon^{-5}; c_V = -3M\varepsilon^{-4}; \\ c_J &= 4 - q[5(\tilde{m}^2 - M^2) + 8\tilde{m}(\tilde{m} - M)]; \\ c_K &= -2qM^2; \quad c_N = -2q\tilde{m}M. \end{aligned} \quad (64)$$

Generally the Hessian have four different eigenvalues:⁴³

$$\lambda^{(1,2)} = c_+ + \frac{1}{2} \left(c_J + 4c_N \pm \sqrt{c_J(c_J + 8c_V + 8c_N)} \right); \quad \lambda^{(3)} = c_+, \lambda^{(4)} = c_- \quad (65)$$

Note that there are new matrices like I_+, I_- when $q \neq 0$. In the case of $q = 0$, $c_+ = c_-$, so that only operator $I = I_+ + I_-$ appears in this case. Actually there is $\lambda^{(4)}$ which is the eigenvalue of Hessian on the antisymmetric matrices. However $\lambda^{(4)} = c_- \geq 0$ is always hold on the RS solutions so that it can be ignored in determining the instabilities of those RS solutions. Since the stability analysis is quite complicated, we divide it into several stages of increasing complexity.

3. Stability of the states on the diagonal - off diagonal "transition" line

The easiest way to see that the RS solutions can be unstable is to look first at the transition line a_T^d , eq.(60). On the transition line one has

$$c_{\pm} = c_U = c_V = c_N = 0; \quad c_J = 4 - 13q^{3/5}; \quad (66)$$

and the eigenvalues simplify to

$$\lambda^{(3)} = 0; \quad \lambda^{(1,2)} = 4 - 13q^{3/5}. \quad (67)$$

Therefore it is unstable for $q > q^t$

$$q^t = \left(\frac{4}{13} \right)^{5/3}, \quad (68)$$

marginally stable at a single point

$$a_T^t = -\frac{28}{13} \left(\frac{13}{4} \right)^{1/3} \approx -3.2 \quad (69)$$

and stable for $q < q^t$. We studied numerically the stability on both sides of this line, see Fig.2. The diagonal (liquid) solution is stable below the line ($a_T^d = 2(3q^{2/5} - 2q^{-1/5})$) for $q > q^t$. The line when $q > q^t$ the phase transition line (liquid to glass) is changed to a different line which will be discussed in the next subsection.

4. Stability of the diagonal solution

Equation for \tilde{m} , coefficients in Hessian and eigenvalues are:

$$-\tilde{m}^{-2} + a_T + 4\tilde{m} - 5q\tilde{m}^3 = 0; \quad (70)$$

$$\begin{aligned} c_+ &= 2\tilde{m}^{-3} - 2q\tilde{m}^2; \quad c_J = 4 - 13q\tilde{m}^2; \\ \lambda^{(1,3)} &= c_+; \quad \lambda^{(2)} = c_+ + c_J = 4 + 2\tilde{m}^{-3} - 15q\tilde{m}^2. \end{aligned} \quad (71)$$

While $\lambda^{(1)}$ is positive, $\lambda^{(2)}$ is positive only below the line defined parametrically via

$$a_T = \frac{5 - 8\tilde{m}^3}{3\tilde{m}^2}; \quad q = \frac{4\tilde{m}^3 + 2}{15\tilde{m}^5}, \quad (72)$$

marked by dotted line in Fig.2. and this line is the phase transition line (liquid to glass) when $q > q^t$. The former diagonal - off diagonal line above the tricritical point is not a phase transition and is left as a light dashed line to show that slope of the line below tricritical point and that of the real transition line is different. It turns out that the line of eq.(72) is a transition line into a RSB state, namely the irreversibility line.

5. Stability of the off diagonal solution

The equations take a form:

$$-\varepsilon^{-2} + a_T + 4\tilde{m} - q [5\tilde{m}^3 - M^3 - 2M^2\tilde{m} - 2\tilde{m}^2M] = 0 \quad (73)$$

$$2\varepsilon^{-3} - q (M^2 + 2\tilde{m}^2) = 0. \quad (74)$$

The coefficients in the expansion of Hessian are: Unlike the case of the $|\psi|^2$ disorder, $\lambda^{(1)} < 0$ for each such a solution. Therefore the diagonal state directly goes over into a RSB glass state. It follows however two lines. The eq.(72) above the tricritical point and eq.(60) below it, see Fig. 2.

VI. RSB IN THE GENERAL CASE

A. General hierarchical gaussian variational Ansatz

The free energy

$$\frac{f}{2n} = \sum_a \left\{ (m^{-1})_{aa} + a_T m_{aa} + 2(m_{aa})^2 \right\} - \sum_{a,b} \left\{ 2rm_{ab}^2 - \frac{q}{4}(m_{ab}^4 + 4m_{aa}m_{bb}m_{ab}^2) \right\} \quad (75)$$

lead on the replica symmetric sector to the following equations:

$$-\varepsilon^{-2} + a_T + 4\tilde{m} - 2r\varepsilon - q[5\tilde{m}^3 - M^3 - 2M^2\tilde{m} - 2\tilde{m}^2M] = 0, \quad (76)$$

$$M[2\varepsilon^{-3} - 2r - q(M^2 + 2\tilde{m}^2)] = 0.$$

For the diagonal solution $M = 0$ one obtains

$$-\tilde{m}^{-2} + a_T + 4\tilde{m} - 2r\tilde{m} - 5q\tilde{m}^3 = 0. \quad (77)$$

The off diagonal solution on the bifurcation line obeys

$$\tilde{m}^{-3} - r - q\tilde{m}^2 = 0. \quad (78)$$

Hessian for the general RS solution takes a form of eq.(62) with coefficients

$$\begin{aligned} c_+ &= 2\varepsilon^{-3} - 2r - q(3M^2 + 2\tilde{m}^2); & c_- &= 2\varepsilon^{-3} - 2r - q(M^2 + 2\tilde{m}^2); \\ c_U &= 4M^2\varepsilon^{-5}; & c_V &= -3M\varepsilon^{-4}; & c_K &= -2qM^2; \\ c_N &= -2q\tilde{m}M; & c_J &= 4 - q[5(\tilde{m}^2 - M^2) + 8\tilde{m}(\tilde{m} - M)]. \end{aligned} \quad (79)$$

On the bifurcation line it simplifies:

$$c_{\pm} = 2\tilde{m}^{-3} - 2r - 2q\tilde{m}^2; c_U = c_V = c_K = c_N = 0; c_J = 4 - 13q\tilde{m}^2. \quad (80)$$

The eigenvalues are

$$\lambda^{(1,2)} = c_{\pm}; \quad \lambda^{(3)} = c_+ + c_J. \quad (81)$$

Therefore the Hessian vanishes $\lambda^{(1,2)} = \lambda^{(3)} = 0$ for the tricritical (branch) point defined by

$$r = \left(\frac{13q}{4} \right)^{2/3} - \frac{4}{13}. \quad (82)$$

Stability of the diagonal solution Hessian and eigenvalues in this case are:

$$\begin{aligned} c_{\pm} &= 2\tilde{m}^{-3} - 2r - 2q\tilde{m}^2; & c_J &= 4 - 13q\tilde{m}^2; \\ \lambda^{(1,2)} &= c_{\pm}; & \lambda^{(3)} &= c_{\pm} + c_J = 4 + 2\tilde{m}^{-3} - 2r - 15q\tilde{m}^2. \end{aligned} \quad (83)$$

Below the tricritical point we solve equation $\lambda^{(1)} = 0$ perturbatively in q :

$$\tilde{m} = r^{-1/3} \left(1 - \frac{q}{3}r^{5/3} \right) + O(q^2) \quad (84)$$

and substitute \tilde{m} into eq.(77) to determine the "weak disorder" part of the glass transition line:

$$a_T^{g1} = -\frac{4-r}{r^{1/3}} + \left(\frac{5}{r} + \frac{4r^{4/3}}{3} \right) q + O(q^2). \quad (85)$$

Above the tricritical point, namely for larger disorder, one solves the equation $\lambda^{(3)} = 0$ perturbatively in q around the tricritical point of eq.(82), $q^t(r) = \frac{4}{13} \left(r + \frac{4}{13}\right)^{3/2}$:

$$\tilde{m} = \left(r + \frac{4}{13}\right)^{-1/3} \left(1 - \frac{10}{24 + 13r} \Delta\right) + O(\Delta^2); \quad \Delta = \frac{q}{q^t(r)} - 1. \quad (86)$$

The NEA RS solution is unstable everywhere as $c_+ < 0$ ($c_+ < c_- = 0$). We therefore obtain the glass transition line with RSB in the general case. To compare it with experiment one has to specify phenomenologically the precise dependence of the GL model parameters on temperature. Next section is devoted to this.

VII. COMPARISON OF THE THEORETICAL AND THE EXPERIMENTAL PHASE DIAGRAMS

A. General picture and comparison with other theories

As was discussed in Introduction, the interplay between disorder and thermal fluctuations makes the phase diagram of high T_c superconductors very complicated. As a result of the present investigation together with the preceding one¹³ regarding the order - disorder transition the following qualitative picture of the $T - H$ phase diagram of a 3D superconductor at temperatures not very far from $H_{c2}(T)$ (so that the LLL approximation is valid) emerges, see schematic diagram Fig. 3. There are two independent transition lines.

1. The positional order-disorder line.

The unified first order universal order - disorder line comprising the melting and the second peak sections separates the homogeneous and the crystalline (Bragg) phases. The transition is therefore defined by the translation and rotation symmetry only, and the intensity of the first Bragg peak can be taken as order parameter. The broken symmetry is not directly related to pinning, however the location of the line is sensitive to disorder. One sees on Fig.3 that as the disorder strength n increases the melting line (solid line) curves down at lower point merging with the second peak segment. The effect of disorder is quite minor in the high temperature region, in which the thermal fluctuations dominate, but become dominant at low temperatures. The line makes a wiggle near the experimentally claimed critical point. The “critical point” is reinterpreted¹³ as a (noncritical) Kauzmann point in which the latent heat vanishes and the line is parallel to the T axis in the low temperature region. The surprising “wiggle”, which appears in 3D only, has actually been observed in some experiments.¹⁴ It is located precisely in the region in which the thermal fluctuations and the disorder compete. One might expect that the line just has a maximum like in *BSCCO*, but the situation might be more complex. Thermal fluctuations, on the one hand side, make the disorder less effective, the less disorder effect will favor solid, but, on the other hand side, they themselves melt the solid. The theoretical magnetization, the entropy and the specific heat discontinuities at melting line¹³ compare well with experiments^{3,12}. The low temperature segment of the disorder dominated second peak line is weakly temperature dependent. Its field strongly decreases as the disorder strength increases.

2. The glass transition line.

The second line is the glass transition line, the dashed line in Fig.3. We assume very small q and draw on Fig.3 the glass lines for three different values of n . One observes as expected, that, as the disorder strength increases, the line moves towards higher temperatures. We have not calculated the glass line in the crystalline state, but anticipate that it depends little on the crystalline order. This is consistent with observations made in Ref. 33 in which it was noticed (in a bit different context of layered materials and columnar defects) that lateral modulation makes a very small difference to the glass line although it is obviously very important for the location of the order - disorder line. So we just continue the glass line in the homogeneous phase into the crystalline side (still marking it by a dotted lines). If the glass lines of the liquid side and solid side join to a single glass line, then the glass line must cross the ODT line right at the Kauzmann point. The theoretical calculated intersection point in Fig. 3 marked by black blob do not appear at the Kauzmann point. We attribute this to different approximations made to draw the ODT and GT line. That the glass line crosses the ODT line right at the Kauzmann point has been indeed supported by some evidences in an experiment in *BSCCO*¹⁷, thought two lines crossing exactly at the Kauzmann point or not is still an open question experimentally and theoretically.

Consequently there are four different phases, see Fig. 4: pinned solid (= Bragg glass), pinned liquid (=vortex glass), unpinned solid (or simply solid) and unpinned liquid (or simply liquid). The four phases of the vortex matter are also expected to be present in the case of layered quasi 2D superconductors and it was shown by in *BSCCO* in

17 that the conductivity and the magnetization both indicate the glass line crossing the ODT line near the maximum (Kauzmann point). There is evidence of the crossing of the ODT and GT line also in *LaSCCO*¹⁸ and *YBCO*^{12,16}, but the line seems to lie very close to the melting line (the segment of ODT line in the high temperature). In Ref. 16 a great care was paid to distinguish the two lines, and it was found that at low field the GT line crosses again the melting line so that the lower field segment of the melting line is again separating two glassy or pinned states.

Now we compare the results on the phase diagram with other theories. The only known theory providing both the ODT and the glass lines is the density functional model. The picture advocated in Ref. 28 on basis of the replica density functional calculation in the framework of thermodynamics of pinned line objects is qualitatively different from the present one. In this theory the glass line does not intersect the ODT line and therefore there is no unpinned solid phase. The comparison of the theory studied in this paper with the replica density functional theory is complicated by the fact that the applicability ranges of two theories are different. In addition there are other phenomenological approaches, most notably that of ref.⁴⁴, based on Lindermann criterion to map the ODT line.

B. Application to optimally doped YBCO

We plot the ODT and the glass transition line in Fig. 5 along with the experimental data on optimally doped *YBCO* of Ref. 12. The theoretical lines use the fitting parameters of ref. 13 which fitted the ODT line and assume the $|\psi|^4$ disorder strength q is small. We believe the value of this parameter should be measured directly using a replica symmetry breaking dynamical phenomenon rather than fitted in thermodynamics, though it might be possible to adjust q , so that the curve can fit the glass transition line better than the case of $q = 0$. As was argued in 13 (and found to be consistent with experiments on the ODT line and the magnetization, entropy and specific heat discontinuities at melting line) that the general dependence of the disorder strength on temperature near T_c is: $r(t) = n(1-t)^2/t$ with $n = 0.12$. The formula interpolates the one used at lower temperatures in ref. 37 with our dimensionless pinning parameter n (proportional to the pinning centers density) related to the “pinning strength” of Blatter *et al*³⁷ by $n = \gamma\gamma_T^0/\pi G t^{1/2} \xi^3$. Note that experimentally the glass transition line at lower fields is not measured precisely. Different experiments locate it at various places using different criteria. As mentioned above experimentally the GT line often crosses the melting line again at very low fields. This question perhaps cannot be addressed within the lowest Landau level approximation valid at fields above 1kG. The ODT line in the melting region is very well established experimentally by great variety of techniques. However the “second peak” segment is only poorly determined due to difficulty to define it in the essentially dynamic magnetization loops analysis. Recently developed muon spin rotation and neutron scattering methods might be very helpful in that respect.

VIII. SUMMARY

To summarize we considered the effects of both thermal fluctuations and disorder in the framework of the GL approach using the replica formalism. Flux line lattice in type II superconductors undergoes a transition into three “disordered” phases: vortex liquid (not pinned), homogeneous vortex glass (the pinned liquid or the vortex glass) and the Bragg glass (pinned solid) due to both thermal fluctuations and random quenched disorder. We show that the disordered Ginzburg – Landau model (valid not very far from H_{c2}) in which only the coefficient of a term quadratic in order parameter ψ is random, first considered by Dorsey, Fisher and Huang, leads to a state with nonzero Edwards – Anderson order parameter, but this state is still replica symmetric. Namely there is no ergodicity breaking and no multiple time scales in dynamics are expected. However, when the coefficient of the quartic term in ψ in the GL free energy also has a random component, replica symmetry breaking effects appear (with ergodicity breaking). The location of the glass transition line in 3D materials is determined and compared to experiments. The line is clearly different from both the melting line and the second peak line describing the translational and rotational symmetry breaking at high and low temperatures respectively. The phase diagram is therefore separated by two lines into four phases mentioned above. In principle we could obtain the RSB solution near the phase transition line by expanding the equations around the phase transition line as in the spin glass theory, see, for example ref. 34, and we found that the RSB is continuous. Thus RSB states involve multiple time scales in relaxation phenomena.

It is natural to expect and is confirmed that the glass (irreversibility) line crosses the “order – disorder” line not very far from its Kauzmann point. We are not sure if the crossing is right at Kauzmann point. If two GT lines (on liquid side and solid side) are joined, the crossing must be right at the Kauzmann point. We believe (speculate)

that the glass line should cross the “order - disorder” line right at the Kauzmann point if the experiments can be done accurately and the theory shall confirm it if the model can be solved exactly. It is of great interest to solve a solvable toy model to test this idea. The Kauzmann point is a point in which the magnetization and the entropy difference between solid and liquid phases changes sign. In this region the positive slope disorder dominated second peak segment joins the thermal fluctuations dominated negative slope melting segment. This is the region in which effects of the disorder and of the thermal fluctuation are roughly of the same strength.

The replica symmetry breaking solution found here can be used to calculate the detailed properties inside the glass state. This however require generalization of the theory to include dynamics, since most of irreversible phenomena are time dependent. In particular it would be interesting to estimate the time scales associated with quenched disorder. This is left for a future work. Also we have considered only the three dimensional GL model here. It can be applied to superconductors with rather small anisotropy. It would be interesting to generalize the calculation to the Lawrence - Doniach model and to the two dimensional case describing thermal fluctuations and disorder in more anisotropic layered superconductors and thin films..

Acknowledgments

We are grateful to E.H. Brandt, B. Shapiro, A. Grover, E. Andrei, F. Lin, J.-Y. Lin and G. Bel for numerous discussions, T. Nishizaki, E. Zeldov and Y. Yeshurun, L. Paulus for providing details of their experiments sometimes prior to publications. The work was supported by NSC of Taiwan grant. The work of BR was supported by NSC of Taiwan grant NSC#93-2112-M-009-023 and the work of DL was supported by the Ministry of Science and Technology of China (G1999064602) and National Nature Science Foundation (#10274030). B.R. is very grateful for Weizmann Institute of Science for warm hospitality during sabbatical leave.

¹ For a review on the vortex phase diagram, see P. Gammel, D.A. Huse, and D.J. Bishop, in “Spin Glasses and Random Fields”, edited by A.P. Young, World Scientific (1998) and references therein.

² D.R. Nelson, Phys. Rev. Lett. **60**, 1973 (1988).

³ F. Bouquet, C. Marcenat, E. Steep, R. Calemczuk, W.K. Kwok, U. Welp, G.W. Crabtree, R.A. Fisher, N.E. Phillips, and A. Schilling, Nature **411**, 448 (2001).

⁴ T. Giamarchi , P. Le Doussal, Phys. Rev. Lett. **75**, 3372 (1994); Phys. Rev. **B52**, 1242 (1995).

⁵ D. Ertas and D.R. Nelson, Physica **C272**, 79 (1996).

⁶ Y. Nonomura and X. Hu, Phys. Rev. Lett. **28**, 5140 (2001).

⁷ E. Zeldov, D. Majer, M. Konczykowski, V.B. Geshkenbein, V.M. Vinokur, and H. Shtrikman, Nature **375**, 373 (1995); R. Liang, D.A. Bonn, W.N. Hardy, Phys. Rev. Lett. **76**, 835 (1996).

⁸ A. Schilling, R.A. Fisher, N.E. Phillips, U. Welp, D. Dasgupta, W.K. Kwok, and G.W. Crabtree Nature **382**, 791 (1996); M. Roulin, A. Junod, E. Walker, Science **273**, 1210 (1996).

⁹ B. Khaykovich, E. Zeldov, D. Majer, T. W. Li, P. H. Kes, and M. Konczykowski, Phys. Rev. Lett. **76**, 2555 (1996).

¹⁰ Y. Radzyner, A. Shaulov, Y. Yeshurun, Phys. Rev. **B65**, 100513 (R) (2002); Y. Radzyner, A. Shaulov, Y. Yeshurun, I. Felner, K. Kishio, and J. Shimoyama, Phys. Rev. **B65**, 100503 (R) (2002).

¹¹ N. Avraham, B. Khaykovich, Y. Myasoedov, M. Rappaport, H. Shtrikman, D.E. Feldman, T. Tamegai, P.H. Kes, M. Li, M. Konczykowski, K. van der Beek, and E. Zeldov, Nature **411**, 451 (2001).

¹² N. Kobayashi, T. Nishizaki, K. Shibata, T. Sato, M. Maki, and T. Sasaki, Physica **C362**, 121 (2001); K. Shibata, T. Nishizaki, T. Sasaki, and N. Kobayashi, Phys. Rev. **B66**, 1214518 (2002).

¹³ D. Li and B. Rosenstein, Phys. Rev. Lett. **90**, 167004 (2003).

¹⁴ D. Pal, S. Ramakrishnan, A. K. Grover, D. Dasgupta, and Bimal K. Sarma, Phys. Rev. **B63**, 132505 (2001); D. Pal , S. Ramakrishnan, and A. K. Grover, Phys. Rev. **B65**, 096502 (2002).

¹⁵ K. Deligiannis, M. Charalambous, J. Chaussy, R. Liang, D. Bonn, and W.N. Hardy, Physica **C341**, 1329 (2000).

¹⁶ B.J. Taylor, S. Li, M.B. Maple and M.P. Maley, Phys. Rev. **B68**, 054523 (2003).

¹⁷ D. T. Fuchs, E. Zeldov, T. Tamegai, S. Ooi, M. Rappaport, and H. Shtrikman, Phys. Rev. Lett. **80**, 4971 (1998); E. Zeldov private communication.

¹⁸ U. Divakar, A.J. Drew, S.L. Lee, R. Gilardi, J. Mesot, F.Y. Ogrin, D. Charalambous, E.M. Forgan, G.I. Menon, N. Momono, M. Oda, C.D. Dewhurst, and C. Baines, Phys. Rev. Lett. **92**, 237004 (2004).

¹⁹ V. Dotseko, “An Introduction to the Theory of Spin Glasses and Neural Networks”, Cambridge University Press (2001).

²⁰ M.P.A. Fisher, Phys. Rev. Lett. **62**, 1415 (1989); D.S. Fisher, M.P.A. Fisher and D.A. Huse, Phys. Rev. **B43**, 130 (1991).

²¹ T.Natterman, Phys. Rev. Lett. **64**, 2454 (1990); T. Natterman and S. Scheindl, Adv. Phys. **49**, 607 (2000).

²² P. Olsson and S. Teitel, Phys. Rev. Lett. **87**, 1370001 (2001).

²³ T. Giamarchi, and S. Bhattacharya, In “High Magnetic Fields: Applications in Condensed Matter Physics and Spectroscopy”, p.314, ed. C. Berthier *et. al.*, Springer-Verlag, 2002.

²⁴ H.K. Bokil and A.P. Young, Phys. Rev. Lett. **74**, 3021 (1995).
²⁵ A. van Otterlo, R.T. Scalettar, G.T. Zimanyi, Phys. Rev. Lett. **81**, 1497 (1998).
²⁶ C. Reichhardt, A. van Otterlo, G.T. Zimanyi, Phys. Rev. Lett. **84**, 1994 (2000).
²⁷ S. E. Korshunov, Phys. Rev. **B48**, 3969 (1993).
²⁸ G.I. Menon, Phys. Rev. **B65**, 104527 (2002).
²⁹ E.H. Brandt, Reports on Progress in Physics **58**, 1465 (1995).
³⁰ D.J. Thouless, Phys. Rev. Lett. **34**, 946 (1975); E. Brezin, D. R. Nelson, A. Thiaville, Phys. Rev. **B31**, 7124 (1985).
³¹ A.T. Dorsey, M. Huang, and M.P.A. Fisher, Phys. Rev. **B45**, 523 (1992).
³² H. Sompolinsky and A. Zippelius, Phys. Rev. **B25**, 6860 (1982).
³³ Z. Tesanovic and I. F. Herbut, Phys. Rev. B 50, 10389 (1994).
³⁴ G. Parisi, J. Phys. **A13**, 1101 (1980).
³⁵ D. Li, B. Rosenstein, Phys. Rev. Lett. **86**, 3618 (2001); Phys. Rev. **B65**, R220504, 024514 (2002).
³⁶ A. Schilling, U. Welp, W.K. Kwok, and G.W. Crabtree, Phys. Rev. **B65**, 054505 (2002).
³⁷ G. Blatter, M.V. Feigel'man, V.B. Geshkenbein, A.I. Larkin, and V.M. Vinokur, Rev. Mod. Phys. **66**, 1125 (1994).
³⁸ G.I. Menon and C. Dasgupta, Phys. Rev. Lett. **73**, 1023 (1994); G.I. Menon, C. Dasgupta, and T. V. Ramakrishnan, Phys. Rev. **B60**, 7607 (1999).
³⁹ G.J. Ruggeri and D.J. Thouless, J. Phys. **F6**, 2063 (1976); Z. Tesanovic and A. V. Andreev, Phys. Rev. **B49**, 4064 (1994); R. Săsik and D. Stroud, Phys. Rev. Lett. **75**, 2582 (1995).
⁴⁰ T. Giamarchi, P. Le Doussal, Phys. Rev. **B53**, 15206 (1996); Phys. Rev. **B55**, 6577 (1997).
⁴¹ M. Mezard and G. Parisi, J. Phys. (France) **I 1**, 809 (1991).
⁴² Z. L. Xiao, E.Y. Andrei, and M.J. Higgins, Phys. Rev. Lett. **83**, 1664 (1999); Y. Paltiel, E. Zeldov, Y.N. Myasoedov, H. Shtrikman, S. Bhattacharya, M.J. Higgins, Z.L. Xiao, E.Y. Andrei, P.L. Gammel and D.J. Bishop, Nature **403**, 398 (2000); Y. Paltiel, E. Zeldov, Y. Myasoedov, M. L. Rappaport, G. Jung, S. Bhattacharya, M.J. Higgins, Z.L. Xiao, E.Y. Andrei, P.L. Gammel and D.J. Bishop, Phys. Rev. Lett. **85**, 3712 (2000); X.S. Ling, S. R. Park, B.A. McClain, S.M. Choi, D.C. Dender and J.W. Lynn, Phys. Rev. Lett. **86**, 712 (2001); Z.L. Xiao, O. Dogru, E.Y. Andrei, P. Shuk and M. Greenblatt, Phys. Rev. Lett. **92**, 227004 (2004).
⁴³ J.R.L. de Almeida and D.J. Thouless, J. Phys. **A11**, 983 (1978).
⁴⁴ G.P. Mikitik, E.H. Brandt, Phys. Rev. **B64**, 184514 (2001); J. Kierfeld, V. Vinokur, Phys. Rev. **B61**, R14928 (2000).

Figure captions

Fig. 1

Schematic $a_T - r$ plane phase diagram of the vortex liquid with the $|\psi|^2$ disorder only. a_T is the LLL scaled temperature, while r is the $|\psi|^2$ disorder strength. The dotted line in the is the glass transition line. Below the line, the state is described by a replica diagonal matrix $m_{ab} = m\delta_{ab}$, while above line the vortex state has a nonzero Anderson Edwards parameter.

Fig. 2

Phase diagram with the $|\psi|^4$ disorder only in the $a_T - q$ plane. The dotted line marks the replica symmetry breaking glass transition. The upper part above the "tricritical" point of this line is given by eq.(72), while the lower part below the "tricritical" point of the line is given by eq.(60). The dashed line is also given by eq.(60), but does not correspond to a phase transition line. It is just a bifurcation line between two replica symmetric (the diagonal and the off diagonal) states.

Fig. 3

The $H - T$ Phase diagram for the $|\psi|^2$ disorder only ($q = 0$) for three different disorder strength $n = 0.12, 0.3$ and 0.08 . The dashed dotted line is $H_{c2}(T)$, the dotted line is the glass transition line, the solid line is the order-disorder (ODT or liquid -solid) transition line. Black blobs are the intersection points of the GT and the ODT lines.

Fig. 4

The schematic phase diagram of $YBCO$. Four distinct thermodynamic phases are: PL - pinned liquid (or vortex glass), PS - pinned solid (or the Bragg glass), S - solid (unpinned solid), and L - liquid (unpinned liquid).

Fig. 5

Comparison of the theoretical $YBCO$ phase diagrams with the experiment. The dotted and the solid lines are the theoretical glass transition and the order-disorder transition lines respectively for the disorder strengths $n = 0.12$ and $q = 0$. $H_m(T)$, $H_{sp}(T)$, $H_g(T)$ are the experimental the melting (ref.12), the second peak (ref. 3³), and the glass transition (ref. 12) lines respectively.

IX.

Fig. 1

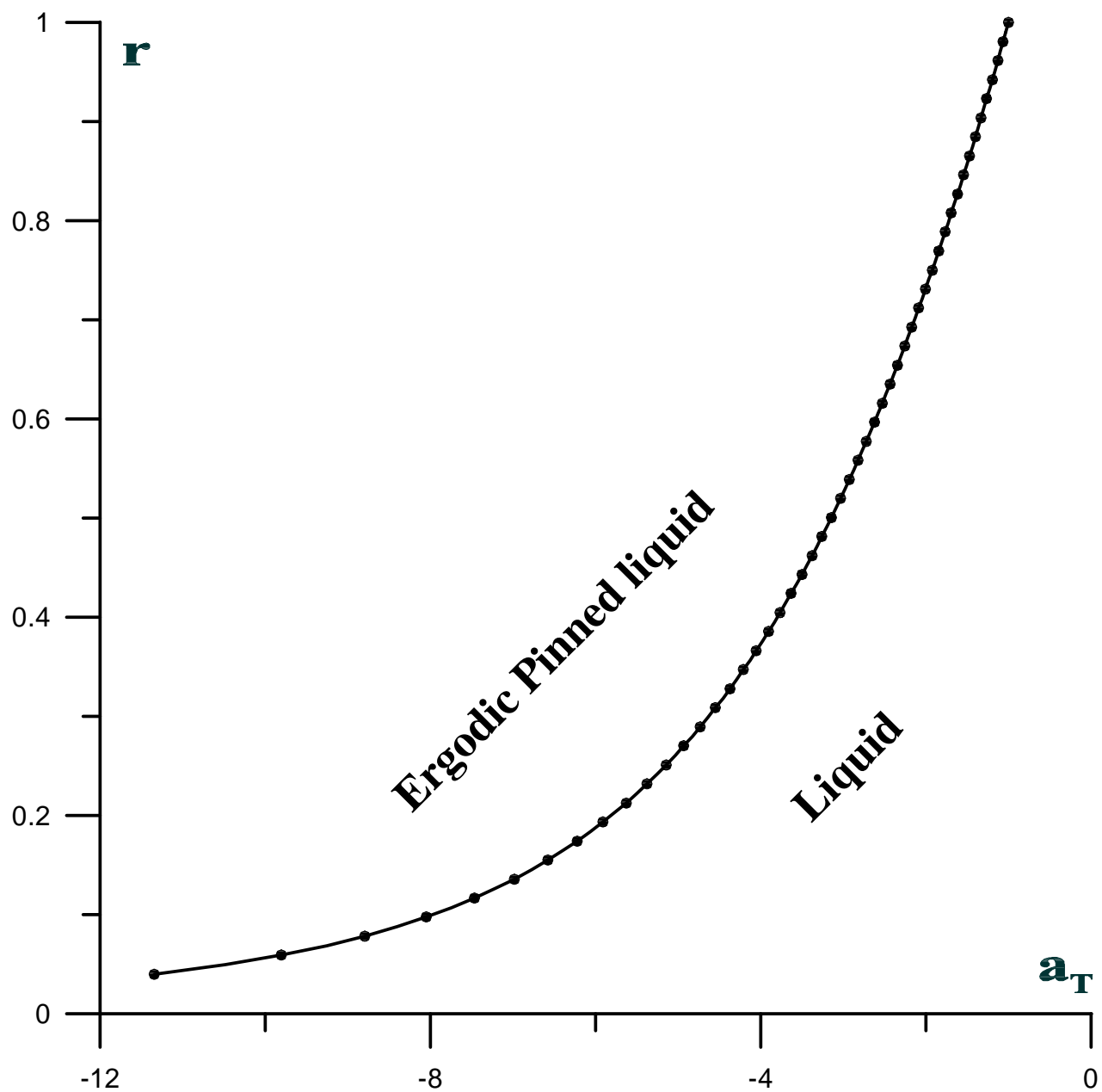


Fig. 2

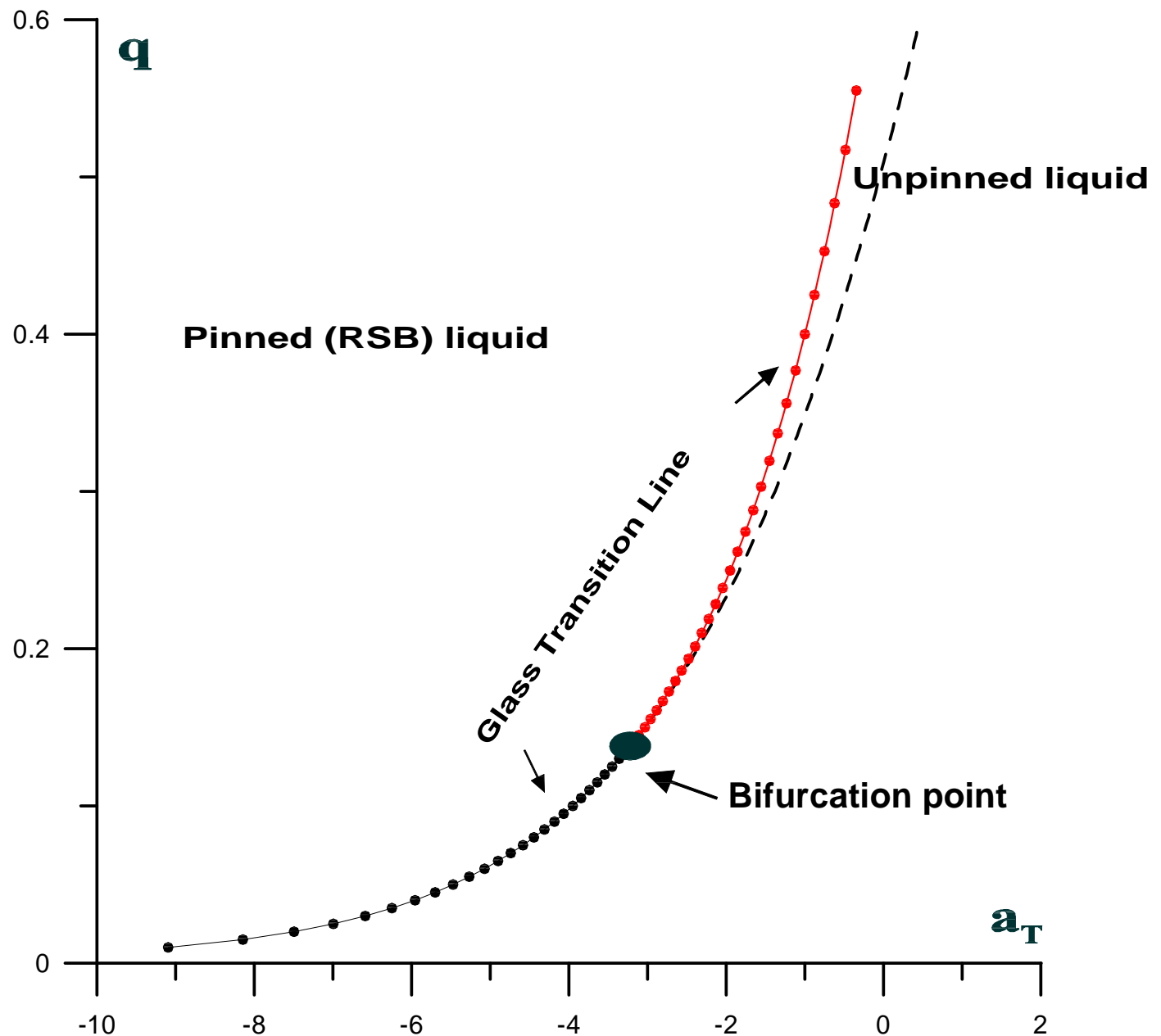


Fig. 3

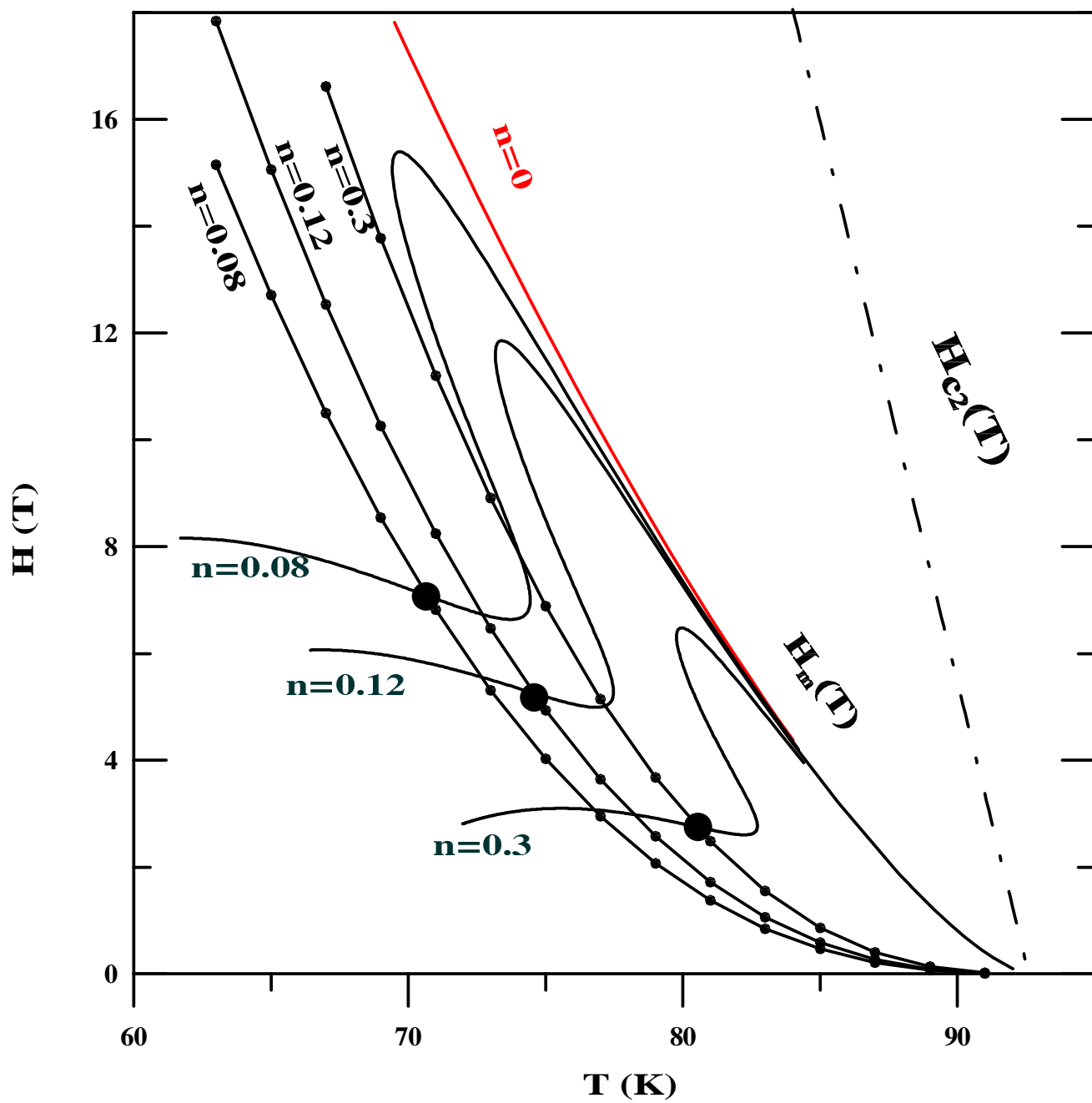


Fig. 4

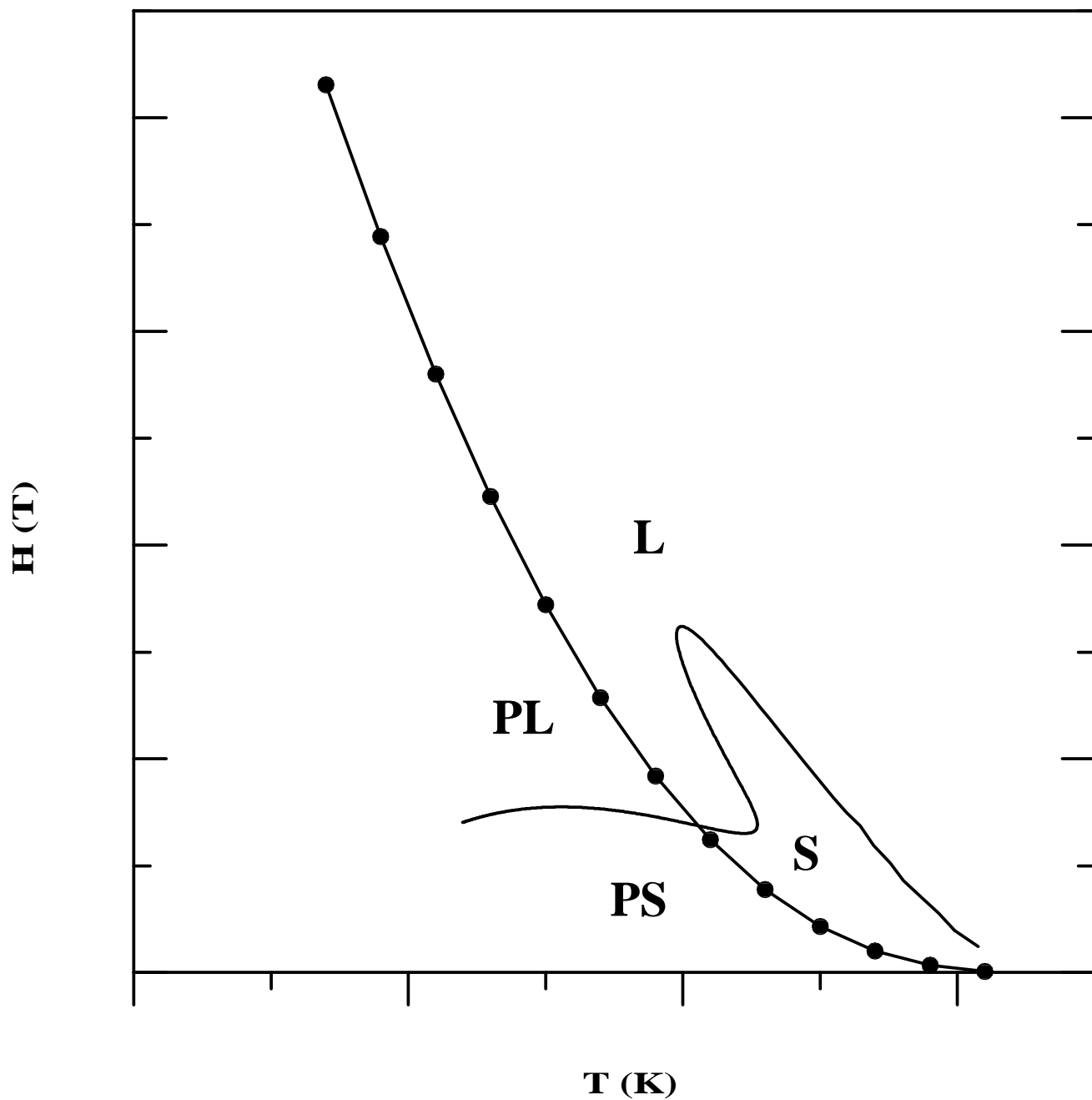


Fig. 5

